

# A new continuous assay for quantitative assessment of enzymatic degradation of poly(ethylene terephthalate) (PET)

**Thomsen, Thore Bach; Schubert, Sune W.; Hunt, Cameron J.; Westh, Peter; Meyer, Anne S.**

*Published in:*
Enzyme and Microbial Technology

*Link to article, DOI:*
10.1016/j.enzmictec.2022.110142

*Publication date:*
2023

*Document Version*
Publisher's PDF, also known as Version of record

Enzyme and Microbial Technology 162 (2023) 110142

Contents lists available at ScienceDirect

Enzyme and Microbial Technology

journal homepage: www.elsevier.com/locate/enzmictec

# A new continuous assay for quantitative assessment of enzymatic degradation of poly(ethylene terephthalate) (PET)

Thore Bach Thomsen [1], Sune W. Schubert [1], Cameron J. Hunt, Peter Westh, Anne S. Meyer [*]

*Department of Biotechnology and Biomedicine, Technical University of Denmark, Søltofts Plads, DK-2800 Kgs. Lyngby, Denmark*

ARTICLE INFO

*Keywords:*
Enzymatic PET degradation
Assay development
PET hydrolase
Biotechnology
Interfacial enzymology
Heterogeneous catalysis

ABSTRACT

Enzymatic degradation of poly(ethylene terephthalate) (PET) has emerged as a promising route for ecofriendly biodegradation of plastic waste. Several discontinuous activity assays have been developed for assessing PET hydrolyzing enzymes, usually involving manual sampling at different time points during the course of the enzymatic reaction. In this work, we present a novel, compartmentalized UV absorbance assay for continuous detection of soluble hydrolysis products released during enzymatic degradation of PET. The methodology is based on removal of the walls separating two diagonally adjacent wells in UV-transparent microplates, to ensure passage of soluble enzymatic hydrolysis products between the two adjacent wells: One well holds an insoluble PET disk of defined dimensions and the other is used for continuous reading of the enzymatic product formation (at 240 nm). The assay was validated by quantifying the rate of mixing of the soluble PET degradation product BHET (bis(2-hydroxyethyl) terephthalate) between the two adjacent wells. The assay validation also involved a simple adjustment for water evaporation during prolonged assays. With this new assay, we determined the kinetic parameters for two PET hydrolases, DuraPETase and $LCC_{ICCG}$, and verified the underlying assumption of steady-state reaction rates. This new continuous assay enables fast exploration and robust kinetic characterization of PET degrading enzymes.

## 1. Introduction

Over the last century, synthetic polymers have become an integral part of modern life due to their versatile and durable properties [1,2]. Accordingly, the production of plastics has increased rapidly, reaching an annual production of 367 Mt in 2020 [3]. This high production has led to an increasing amount of plastic waste, which due to poor collecting rates, poses an ecological challenge due to its accumulation in landfills and marine environments [4].

Although the most widely used plastics are synthetic polymers, new discoveries have shown that microbial enzymes are capable of degrading certain types, notably poly(ethylene terephthalate) (PET) [5–7]. These discoveries have provided a new starting point for enzyme-driven PET recycling [8,9]. The enzymes that are active on PET include certain esterases (EC 3.1.1.1 and EC 3.1.1.2), lipases (EC. 3.1.1.3), cutinases (EC 3.1.1.74), and notably the new class of enzymes categorized as PET hydrolases (PETases) (EC 3.1.1.101) [6,7]. Currently, several efforts focus on discovery, characterization, and protein engineering of PET degrading enzymes [10–12].

Proper performance assessment and comparison of PET degrading enzymes relies on robust and accurate assays. Several different analytical methods have been established for investigating the enzymatic degradation of PET [13]. A few of these assays permit continuous analysis, e.g. involving pH-stat [14], turbidimetry [15], calorimetry [16], or impedance spectroscopy measurement [17]. However, none of these continuous assays fulfill the requirement for assessing the enzymatic degradation of PET in a simple setup that permits small reaction volumes (to test limited amounts of enzymes) and allows for multiple reactions to be run in parallel.

Suspension-based assays that apply UV-absorption spectroscopy to detect the hydrolysis products are among the most commonly used for PET hydrolases [18–20]. The analytical principle of these UV-absorption assays is based on the high absorbance of the phenyl-groups present in the soluble enzymatic degradation products of PET, i.e. terephthalic acid

*Abbreviations:* PET, poly(ethylene terephthalate); BHET, bis(2-hydroxyethyl) terephthalate; MHET, mono(2-hydroxyethyl)terephthalic acid; TPA, terephthalic acid.

* Corresponding author.
*E-mail address:* asme@dtu.dk (A.S. Meyer).

[1] These authors contributed equally to this study.

https://doi.org/10.1016/j.enzmictec.2022.110142
Received 14 August 2022; Received in revised form 1 October 2022; Accepted 12 October 2022
Available online 14 October 2022

(TPA), mono(2-hydroxyethyl)terephthalic acid (MHET), and bis (2-hydroxyethyl)terephthalic acid (BHET) [21,22]. A limitation of the UV absorbance assay is that PET itself absorbs at 240 nm and thus that larger insoluble substrate particles result in light scattering. It is therefore not possible to run the reaction continuously in a plate reader using a standard microplate, as the presence of the PET substrate interferes with the measurement, and the assays must therefore be run discontinuously. Such discontinuous assays usually require a significant amount of diligent manual sampling to attain accurate and comparable results, and since the enzymatic degradation of PET is a slow process that furthermore only slowly achieves a steady-state, especially at increased substrate crystallinity [18,23–25], the sampling usually has to take place over extended time periods.

Here, we demonstrate and validate a compartmentalized UV absorbance assay for continuous detection of soluble hydrolysis products during enzymatic degradation PET, i.e., a continuous assay that can be run in UV-transparent microplates. The applicability of the continuous assay is evaluated through inverse Michaelis-Menten ($^{inv}$MM) kinetics [26] on two thermostable PET degrading enzymes: $LCC_{ICCG}$, a variant of the leaf-branch compost cutinase (LCC) [12], and DuraPETase, a variant of the *Ideonella sakaiensis* PETase [27], and by analyzing the simulated rates of mixing of the hydrolysis products versus the enzyme catalyzed product formation rates.

## 2. Materials and methods

### 2.1. Enzymes

$LCC_{ICCG}$ was heterologously expressed in *E. coli* SHuffle T7 competent cells (New England Biolabs, Ipswich, Massachusetts, USA), while DuraPETase was heterologously expressed in the *E. coli* BL21 (DE3) competent cells (New England Biolabs, Ipswich, MA, USA) as described previously [18].

### 2.2. Substrate

The PET material used as substrate was 1 mm thick amorphous PET sheets (Goodfellow Cambridge Ltd, Huntingdon, UK) (Cat. No. ES303010), punched into uniform disks (Ø=6 mm) using a generic hole punch. In order to remove the enthalpy relaxation caused by ageing of the polymer, the PET disks were annealed at 85 °C for 5 min, and subsequently quenched in ice water for 30 s as described in [25]. The starting crystallinity of this PET material was 9.1 ± 1.3%, as measured by differential scanning calorimetry (DSC) as described earlier [25].

### 2.3. Modification of microplates

To allow for continuous spectrophotometric measurements of product formation resulting from PET hydrolase action, a UV-transparent flat-bottom well microplate (made up of polystyrene with UV-transmissible well bottoms) (Corning Inc., Corning, New York, USA) (Cat. No. 3635) was modified to ensure unrestricted passage of soluble enzymatic hydrolysis products between two diagonally adjacent wells (Fig. 1). The modification involved cautious removal of the interjoining walls of two diagonally adjacent wells using a DREMEL® Rotary Tool (with a 4.8 mm routing bit) (DREMEL, Racine, Wisconsin, USA). During experimental runs, one well contained the PET disk (denoted as the reaction well), while the other well (denoted as the analytical well) was used for continuous UV detection of the soluble PET degradation products formed during reaction. The modified plates were subjected to quality control to ensure that the interconnected wells were not leaking into the neighboring wells of each set of diagonally adjacent set of wells (Supplementary information, Fig. S1).

### 2.4. Continuous activity assays

The continuous assay was used to measure the product formation as a function of time during the action of DuraPETase and $LCC_{ICCG}$, respectively. Each enzyme was added to the connected wells in dosages ranging from 20 nM to 800 nM in 650 μL of 50 mM Glycine-NaOH buffer at pH 9, and preheated at 50 °C for 10 min in an Epoch 2 microplate spectrophotometer (BioTek, Winooski, Vermont, USA). Subsequently, a PET disk was placed into the reaction well and UV absorbance was detected at 240 nm in the analytical well for up to 90 min at intervals of 45 s. A shaking step lasting 3 s was included between each measurement. The UV absorbance of the enzymatic product formation at 240 nm was converted into molar amounts using commercially available BHET as standard. BHET was chosen as the standard since the molar absorption of BHET has been reported to reflect the sum of the pooled absorbance from all soluble PET degradation products [22]. To verify that this also applied under the experimental conditions in this study, we prepared standard curves for both BHET and MHET (Supplementary information, Fig. S2). On this premise, the molar amounts are given in terms of nmol BHET equivalents (BHETeq). Following enzymatic treatment of a PET disk, the reaction mixture was furthermore analyzed using direct light scatter to ensure that no particles were present that could interfere with the light pathway used to detect product formation (data not shown).

For the $^{inv}$MM kinetics analysis, the initial rates, $v_i$, of the PET hydrolase action were determined from the slopes of the progress curves of the enzyme catalyzed reactions achieved at different enzyme dosage levels, $E_0$. The kinetic parameters for interfacially acting enzymes are thus described as the inverse maximal reaction rate, $^{inv}V_{max}$, and the inverse Michaelis-constant, $^{inv}K_M$, respectively, derived as previously described [26], i.e. according to Eq. (1):

$$v_i = \frac{^{inv}V_{max} \cdot E_0}{^{inv}K_M + E_0} \quad (1)$$

### 2.5. Evaporation

Any possible evaporation occurring during the prolonged incubation required for the assay measurements was assessed at 50 °C. This was accomplished by quantifying the residual volume of 650 μL water samples in the microplates after incubation for 0 min, 30 min, 60 min and 120 min. The residual volume was quantified by weighing the

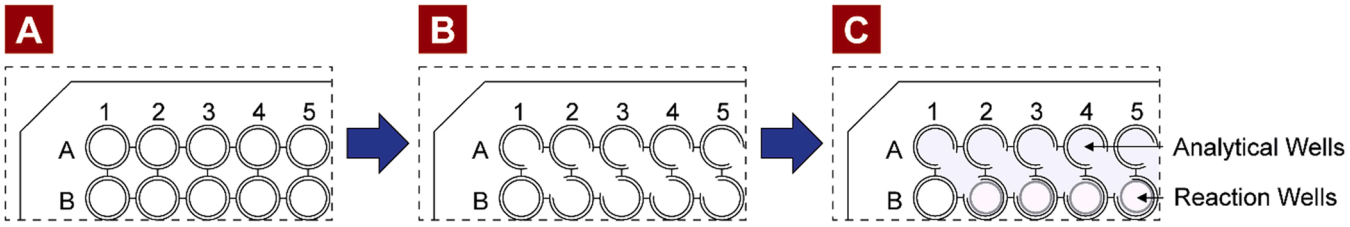


**Fig. 1.** Schematic representation of the modified microplates. A) Standard UV 96-well micrplate. B) Modified microplate used in the continous asssay. The two digonally adjacent wells were conntected by removing the well walls using a DREMEL® Rotary Tool. C) Experimental set-up of the contious assay. Each connected well is filled with an enzyme solution (light blue color). An insoluble PET substrate is added to the reaction well, while the $A_{240}$ is meassured in the analytical well.

remaining water in a connected set of two diagonal wells by pipetting. In addition, the effect of prolonged incubation on the absorbance of a 100 μM BHET solution (650 μL) was evaluated over a 2 h incubation period at 50 °C.

### 2.6. Mixing of BHET between the wells

A study was conducted to quantify the rate of mixing of the soluble hydrolysis products (solutes) in the reaction well and the analytic well. To investigate any potential influence of the presence of the PET disk on the mass transfer of soluble products, the experiment was conducted with and without the presence of a PET disk in the reaction well (Supplementary information, Fig. S3). It was assumed that the mixing of the contents in the reaction- and analytical well can be described as a well-mixed two tank system with a constant molar flow in both directions, i.e. according to the following kinetic scheme (2):

$$n_{rw} \underset{k_r}{\overset{k_f}{\rightleftharpoons}} n_{aw} \tag{2}$$

Here $n_{rw}$ and $n_{aw}$ are the molar amount of solutes in the reaction- and analytical well, while $k_f$ and $k_r$ are the rate constants for the forward and reverse mass flow, respectively. At equilibrium, the concentration of solutes is the same in both wells, thus corresponding to an equilibrium constant equal to 1. Since both wells have the same volume, it follows that the rate constants, $k_f$ and $k_r$, must be the same. Hence, $k_f = k_r = k$. A differential equation of the change in $n_{rw}$ with time, $t$, can be derived from the kinetic scheme in (3):

$$\frac{\Delta n_{aw}}{\Delta t} = k \cdot n_{rw}(t) - k \cdot n_{aw}(t) \tag{3}$$

The $n_{rw}(t)$ at a given time can furthermore be expressed as function of $n_{aw}(t)$:

$$n_{rw}(t) = 2 \cdot n_{eq} - n_{aw}(t) \tag{4}$$

Here $n_{eq}$ is the molar amount in both wells at equilibrium. By adding (4) to (3) and integrating the equation an expression of $n_{aw}(t)$ emerges (Eq. (5)):

$$n_{aw}(t) = n_{eq} + \exp(-2 \cdot k \cdot t) \cdot c \tag{5}$$

Here $c$ is the constant of integration. The rate constant $k$ of the system was quantified by fitting experimental data to (5). A global fit, at which $k$ was fixed, was performed using OriginPro software (OriginLab Corporation, Northampton, Massachusetts, USA). An additional experiment was conducted to verify that the mixing constant of MHET was similar to that of BHET (Supplementary information, Fig. S3).

### 2.7. Simulation of mixing of solutes during enzymatic reactions

The response of the system, was evaluated by simulating the amount of solutes in both wells, coupling (3) with an expression of the change of solutes in the reaction well, which can be described as in Eq. (6):

$$\frac{\Delta n_{rw}}{\Delta t} = V \cdot v + k \cdot n_{aw}(t) - k \cdot n_{rw}(t) \tag{6}$$

Here $V$ denotes the total volume of the connected wells, while $v$ is the product formation rate of the enzymatic reaction occurring in the reaction well. It was assumed that the concentration of substrate was in such excess that $v \approx v_i$ during the course of the reactions included in the simulation.

The product formation rate of the experimental data was then simulated by solving the differential Eqs. (3) - (6) numerically using MATLAB software (MathWorks, Natick, Massachusetts, USA). The observed product formation rates at the linear regions of the progress curves along with the estimated rate constant of the mixing were used as input values in the simulation.

## 3. Results and discussion

### 3.1. Continuous detection soluble products by UV spectrophotometry

The release of soluble products from the hydrolysis of PET using two PET hydrolases, DuraPETase and $LCC_{ICCG}$, was monitored continuously via detection by UV absorption. By connecting two adjacent wells in a microplate by removing the wall structure between two diagonally positioned wells, it was possible to run the enzymatic reaction in the reaction well while detecting the UV absorbance of the supernatant in the analytical well. During enzymatic hydrolysis, the insoluble PET disk was physically retained in the reaction well by the compartmentalized design of the interconnected wells. This compartmentalization prevented any interference to the optical light path used for absorbance measurements in the analytical well. Although one side of the PET disk faced downwards towards the bottom of the microplate, the accessibility of the enzymes to both sides of the substrate PET disk was not restricted (Supplementary information, Fig. S4).

A schematic representation of the plate design is displayed in Fig. 1.

### 3.2. Inverse Michaelis-Menten kinetics of two thermostable PET hydrolases

The performance of the continuous assay was evaluated by quantifying the kinetic parameters ${}^{inv}V_{max}$ and ${}^{inv}K_M$, for both $LCC_{ICCG}$ and DuraPETase. The enzymatic reaction rates at various enzyme concentrations were obtained for each enzyme by monitoring the product formation in the analytical well during enzymatic treatment. Reactions were performed at 50 °C, corresponding to the maximal incubation temperature of the plate reader, and at pH 9, the pH optimum of both $LCC_{ICCG}$ and DuraPETase [18].

The absorbance of a solute measured in the plate reader is only proportional to its concentration within a certain range (i.e. Lambert-Beer's law). The upper detection limit of the product formation, measured by the continuous assay, is therefore limited to the range of this proportionality which corresponded to an upper limit of ~80 nmol BHETeq (Supplementary information, Fig. S2).

The progress curves at various enzyme concentrations of $LCC_{ICCG}$ and DuraPETase are displayed in Fig. 2. A distinct lag phase in the progression of the product formation was observed during the initial treatment (~30–80 min depending on the conditions). After this point, the rate stabilized at a constant, which we define as the initial steady state rate. The rates were converted into μM $min^{-1}$ by dividing the initial rates, determined from Fig. 2A and B, with the starting volume (650 μL).

The estimated rates were plotted against the enzyme concentration (Fig. 3A and B) and fitted to the ${}^{inv}$MM equation, displayed in Eq. 1, to obtain the kinetic parameters, ${}^{inv}V_{max}$ and ${}^{inv}K_M$, listed in Table 1.

No significant difference were observed between the ${}^{inv}K_M$ of $LCC_{ICCG}$ and DuraPETase. These values were in the same range as previously reported ${}^{inv}K_M$ values of other PET degrading enzymes [19,28].

The ${}^{inv}V_{max}$, on the other hand, was more than 6-fold higher for $LCC_{ICCG}$ compared to DuraPETase; the ${}^{inv}V_{max}$ is interpreted as the maximum rate the enzyme can achieve on an insoluble substrate, and implies that all accessible attack sites on the surface of the substrate are constantly occupied by the enzyme. The data verify the applicability of the assay for evaluating kinetics of PET hydrolases. The experimental data show that $LCC_{ICCG}$ outperforms DuraPETase at these reaction conditions even if the optimal reaction temperature for $LCC_{ICCG}$ is in fact 20 °C higher.

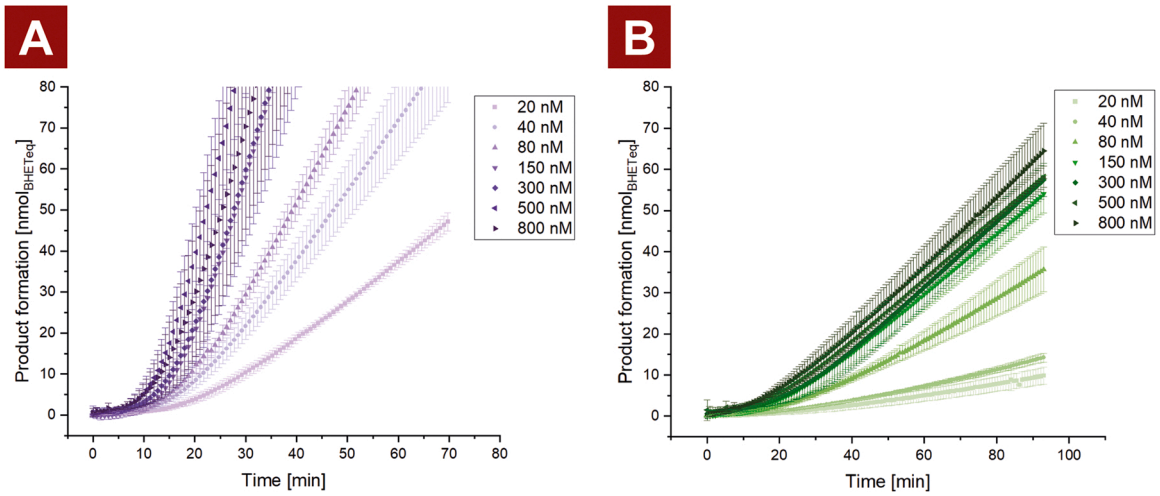


**Fig. 2.** Progress curves at various initial enzyme concentrations (20–800 nM) for A) $LCC_{ICCG}$ and B) DuraPETase. The reactions were performed at 50 °C in 50 mM Glycine-buffer pH 9 for a maximum of 100 min. The data points and error bars represent the average value and standard deviations (n = 3).

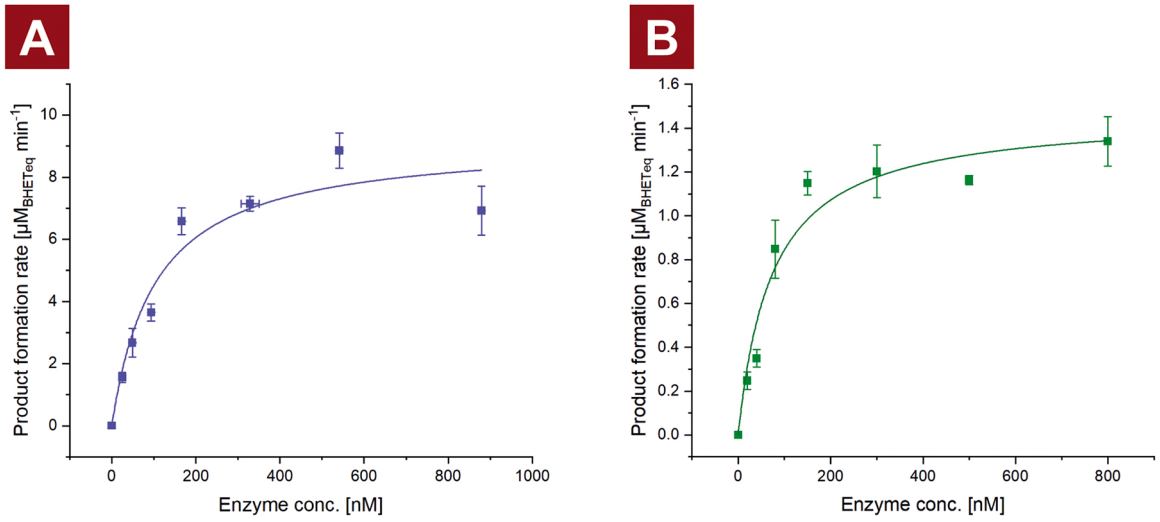


**Fig. 3.** Inverse Michaelis-Menten ($^{inv}$MM) curves of A) $LCC_{ICCG}$ and B) DuraPETase displaying the product formation rates as a function of the enzyme load. The symbols and error bars represent the average and standard deviation (n = 3) of the linear region of the experimental data. The solid lines are non-linear regression fit of the experimental data to the $^{inv}$MM equation (Eq. (1)). The reactions were performed at 50 °C in 50 mM Glycine-buffer pH 9 for a maximum of 100 min. Enzyme dosages and product levels were adjusted to account for water evaporation during the course of reaction.

**Table 1**
Kinetic constants derived from the $^{inv}$MM fits of $LCC_{ICCG}$ and DuraPETase shown in Fig. 3. The values are the fit parameters ± the standard deviation of these based on three replicate measurements for each enzyme. Different superscript letters a and b indicate statistically significant differences between the data for each enzyme ($p < 0.05$), where a is significantly higher than b.

| | $^{inv}K_M$ [nM] | $^{inv}V_{max}$ [μM$_{BHETeq}$ min$^{-1}$] |
|---|---|---|
| $LCC_{ICCG}$ | $104^a \pm 35$ | $9.2^a \pm 0.9$ |
| DuraPETase | $101^a \pm 28$ | $1.5^b \pm 0.1$ |

### 3.3. Validation of the continuous assay

#### 3.3.1. Evaporation

As the continuous assay is an open system, water may evaporate from the wells during incubation in the plate reader. A reduction in the reaction volume is therefore expected to occur during the enzymatic reactions. The evaporation from the interconnected wells was monitored at standard reaction conditions (50 °C over a 2 h incubation period) (Fig. 4A). This corresponded to a linear evaporation rate of 2.15 ± 0.13 μL min$^{-1}$. It can therefore be expected that ~40% of the total reaction volume had evaporated after two hours of incubation. The enzyme concentrations from Fig. 3 A and B were therefore adjusted according to the expected residual volume, at the time at which the rates were calculated. This was done to account for the increasing enzyme concentration caused by evaporation.

The effect of prolonged incubation on the absorbance of reaction products, was evaluated by incubating 72 nmol of BHET at standard conditions (Fig. 4B). A constant signal was observed during the two hours of incubation, despite a ~40% reduction in the sample volume caused by the evaporation. This phenomenon can be explained by the Lambert-Beer's law ($A = C \cdot l \cdot \varepsilon$), as the increase in concentration, ($C$), caused by the reduction in sample volume, is inversely proportional with the length of the optical light path ($l$), at which the absorbance measure is taken.

Threfore, we consider it a fair assumption that the absorbance monitored by the continuous assay is representative with the actual

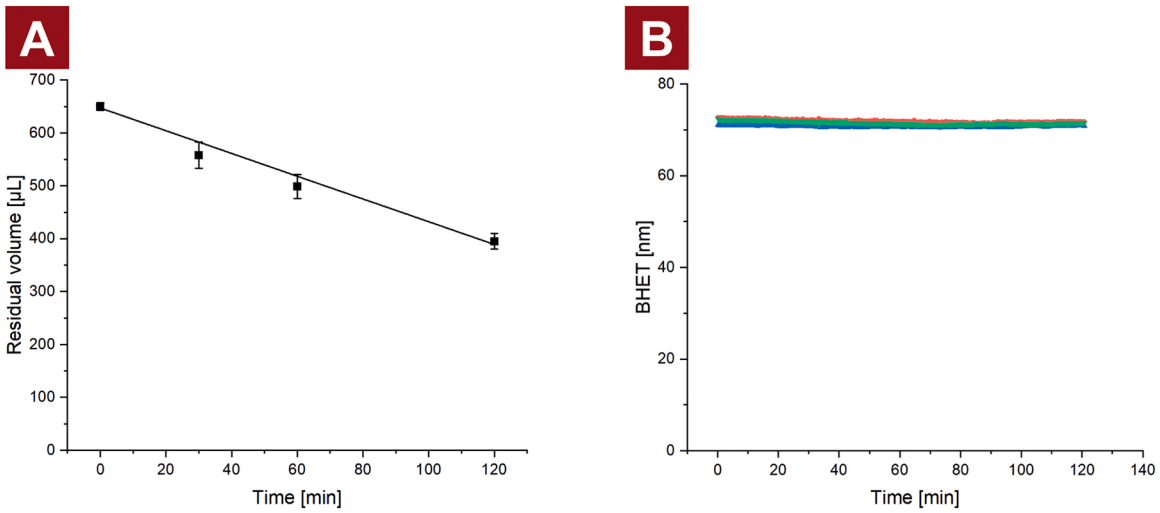


**Fig. 4.** A) Correlation between residual volume of 650 µL water samples and incubation time at 50 °C, the correlation follows a linear trend (y = -(2.15 ± 0.13) x + 647 ± 7, $R^2$ 0.99). The average volume and standard deviation (n = 3) are represented by data points and error bars. B) Change in signal, in nmol BHETeq of three individual samples (represented by red, black, or blue data points) of 72 nmol BHET during 120 min incubation at 50 °C.

molar amount of BHETeq released during the enzyme reaction.

### 3.3.2. *Mixing of solutes between the wells*

A key prerequisite for the continuous assay is that sufficient mixing of contents in the interconnected wells is achieved. We note that the reaction mixture is subjected to physical shaking which dictates that the mass transfer of soluble products between the wells cannot be regarded as diffusion alone, but instead as a combined effect of diffusion and mixing. This will allow the system to obtain a steady-state, at which the product formation rate measured in the analytical well is equal to the rate of the enzymatic reaction in the reaction well.

The rate constant of the mixing was quantified by monitoring the absorbance in the analytical well, after a small amount of a concentrated BHET suspension had been added into the reaction well of individual samples (Fig. 5). The mixing constant of the system was estimated to be 0.247 ± 0.002 $min^{-1}$ using global fitting of the experimental data (Fig. 5) to Eq. (5).

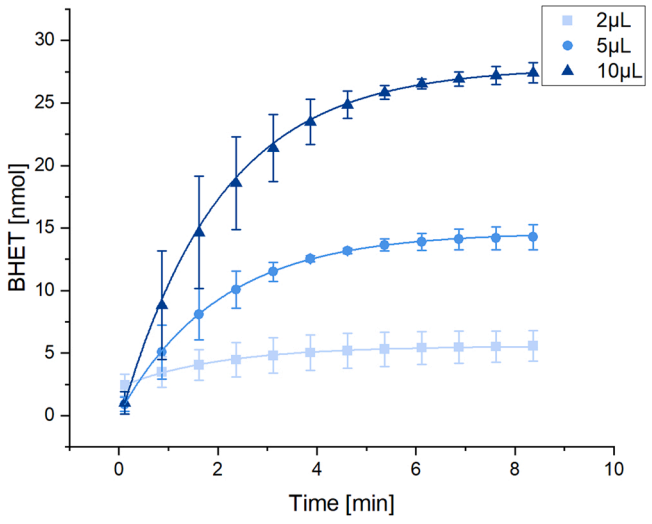


**Fig. 5.** A) Change in BHETeq in the analytical well after adding of three different volumes of a concentrated BHET suspension (2.5 mM) into the reaction well. The average and standard deviation (n = 3) of the experimental data is represented by data points and error bars. The solid lines represent the non-linear global fit of Eq. (5) to the experimental data.

As a consequence of the separation of the reaction well and the analytical well, a delay in the observed product formation rate is expected during the initial incubation. This delay, determined by the mixing rate constant, is equivalent to the time it takes for the detected rate in the analytical well to be equivalent to the product formation rate in the reaction well. The expected product formation measured in the analytical well was simulated using the differential Eqs. (3) and (6) using the estimated rate constant from Fig. 5 and the rate of the linear regions from Fig. 2A and B as input values. This was done to compare the acceleration of the rate observed experimentally with the acceleration associated with the time delay caused by the mixing.

A comparison between the observed and simulated product formation in the analytical well is displayed in Fig. 6A, while the on-set time, defined as the time it takes to reach 95% of the product formation rate at steady state, is displayed in Table 2.

From Fig. 6A it is evident that the reaction rate of the simulated product formation reaches a steady-state after 8 min which, depending on the conditions, was 3.5–10 times faster than the corresponding actual rates. The mixing constant was neither affected by the presence of a PET disk in the reaction well or the type of hydrolysis products (i.e., BHET or MHET) (Supplementary information, Table S1). However, the mixing constant was apparently affected by other parameters, including the specific dimensions of the passage between the interconnected wells in the prepared microplates. As outlined in 2.3 we therefore recommend complete removal of the interjoining walls of two diagonally adjacent wells for successful assay results. The mixing constant used in this study for simulating product formation was conservatively selected to represent the lowest experimental mixing constant obtained throughout our study. The data emphasize the importance of continuous monitoring of the product formation when quantifying the reaction rates, as single end-point measures may result in an underestimation of the rates.

## 4. Conclusion

In order to thoroughly study the characteristics of PET hydrolases, it is important to assess the progression of the rate by which soluble hydrolysis products are released from a PET sample during enzymatic treatment. In this study, we demonstrated the applicability of our continuous activity assay for the quantification of released soluble hydrolysis products from PET disks treated with two PET hydrolases, DuraPETase or $LCC_{ICCG}$.

Both enzymes showed a clear trend where the initial rate increased gradually until a constant rate had been reached. In turn, these constant

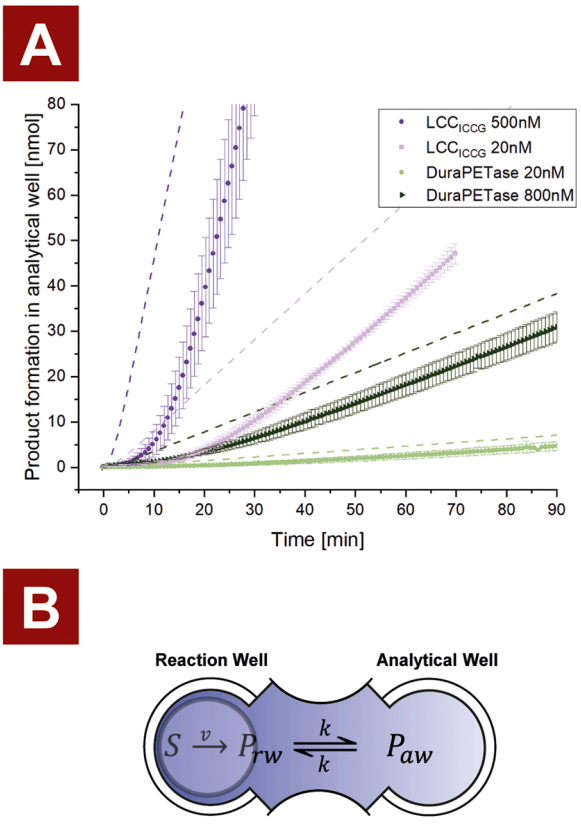


**Fig. 6.** A) Comparison of a simulated product formation (dashed lines) in the analytical well with the experimentally obtained product formation data (progress curves from Fig. 2 (points)). These progress curves include the enzyme loads that correspond to the lowest and highest product formation rates obtained for LCC$_{ICCG}$ (purple) and DuraPETase (green). The simulated progress curves were calculated as the amount of hydrolysis products constrained to the analytical well (V=325 μL). Thus, for comparison, the product formation of the simulated data were multiplied by 2 to adjust for the difference in reaction volume between one and two wells. B) Kinetic reaction scheme used for the simulation model.

**Table 2**
Product formation rates and on-set times for enzymatic reactions achieved at low and high dosage levels of each enzyme, LCC$_{ICCG}$ and DuraPETase. On-set time is defined as the time it takes to reach 95% of the product formation rate for the experimental observation and the simulation of the progress curves (Fig. 6A).

| | **Product formation rate** [nmol min$^{-1}$] | **On-set time Simulated data** [min] | **On-set time Experimental data** [min] |
|---|---|---|---|
| 500 nM LCC$_{ICCG}$ | 5.75 | 8 | 28 |
| 20 nM LCC$_{ICCG}$ | 1.01 | 8 | 56 |
| 800 nM DuraPETase | 0.87 | 8 | 58 |
| 20 nM DuraPETase | 0.16 | 8 | 83 |

rates were used to derive kinetic parameters under the assumption of steady-state kinetics. The results obtained were in line with values reported in the literature. In summary, this continuous activity assay offers a novel tool for further characterization of PET degrading enzymes. The continuous monitoring assay is fast and simple, and has potential as a high-throughput method for kinetic assessment of new putative PET degrading enzymes or engineered PET hydrolases in expression libraries.

As a final remark it is important to state that this assay is not limited to the characterization of PET degrading enzymes, as it can be used to characterize other enzyme working on insoluble substrates. This does only require that the products from enzymatic reactions can be measured by absorbance or other types of optical spectroscopy.

## CRediT authorship contribution statement

**Thore Bach Thomsen:** Conceptualization, Investigation, Methodology, Visualization, Formal analysis, Writing. **Sune W. Schubert:** Conceptualization, Investigation, Methodology, Formal analysis, Writing. **Cameron J. Hunt:** Conceptualization, Methodology, Formal analysis, Funding acquisition, Resources, Writing. **Peter Westh:** Supervision, Funding acquisition. **Anne S. Meyer:** Conceptualization, Project administration, Supervision, Funding acquisition, Resources, Writing.

## Declaration of Competing Interest

There are no competing interest to declare. All authors declare no conflict of interests.

## Data availability

Data will be made available on request.

## Acknowledgments

Funding from The H.C. Ørsted Cofund Postdoc Program, Technical University of Denmark. We also wish to thank Camilo Andres Amaya Chica for excellent technical support during the assay development.

## Appendix A. Supporting information

Supplementary data associated with this article can be found in the online version at doi:10.1016/j.enzmictec.2022.110142

## References

[1] J.H. Lee, K.S. Lim, W.G. Hahm, S.H. Kim, Properties of recycled and virgin poly (ethylene terephthalate) blend fibers, J. Appl. Polym. Sci. 128 (2013) 1250–1256, https://doi.org/10.1002/app.38502.
[2] T. Thiounn, R.C. Smith, Advances and approaches for chemical recycling of plastic waste, J. Polym. Sci. 58 (2020) 1347–1364, https://doi.org/10.1002/pol.20190261.
[3] Plastics Europe Market Research Group (PEMRG), Conversio Market & Strategy GmbH. Plastics Europe Association of Plastics Manufacturers Plastics—The Facts 2021 An analysis of European Plastics Production, Demand Waste Data (2021).
[4] R. Geyer, J.R. Jambeck, K.L. Law, Production, use, and fate of all plastics ever made, Sci. Adv. (2017) 3, https://doi.org/10.1126/sciadv.1700782.
[5] M.A.M.E. Vertommen, V.A. Nierstrasz, M.Van Der Veer, M.M.C.G. Warmoeskerken, Enzymatic surface modification of poly(ethylene terephthalate), J. Biotechnol. 120 (2005) 376–386, https://doi.org/10.1016/j.jbiotec.2005.06.015.
[6] Y. Shosuke, H. Kasumi, T. Toshihiko, T. Ikuo, Y. Hironao, M. Yasuhito, et al., A bacterium that degrades and assimilates poly(ethyleneterephthalate), Science (80-) 351 (2016) 1196–1199.
[7] P.C.F. Buchholz, Golo Feuerriegel, H. Zhang, P. Perez-Garcia, L.-L. Nover, Jennifer Chow, et al., Plastics degradation by hydrolytic enzymes: The plastics-active enzymes database—PAZy, Proteins Struct. Funct. Bioinforma. (2022), https://doi.org/10.1002/PROT.26325.
[8] R. Wei, W. Zimmermann, Microbial enzymes for the recycling of recalcitrant petroleum-based plastics: how far are we? Micro Biotechnol. 10 (2017) 1308–1322, https://doi.org/10.1111/1751-7915.12710.
[9] A. Carniel, V. Waldow, A. de, A.M. de Castro, A comprehensive and critical review on key elements to implement enzymatic PET depolymerization for recycling purposes, Biotechnol. Adv. (2021) 52, https://doi.org/10.1016/j.biotechadv.2021.107811.
[10] H.P. Austin, M.D. Allen, B.S. Donohoe, N.A. Rorrer, F.L. Kearns, R.L. Silveira, et al., Characterization and engineering of a plastic-degrading aromatic polyesterase, Proc. Natl. Acad. Sci. USA 115 (2018) E4350–E4357, https://doi.org/10.1073/pnas.1718804115.
[11] H. Lu, D.J. Diaz, N.J. Czarnecki, C. Zhu, W. Kim, R. Shroff, et al., Machine learning-aided engineering of hydrolases for PET depolymerization, Nat 2022 6047907 604 (2022) 662–667, https://doi.org/10.1038/s41586-022-04599-z.

[12] V. Tournier, C.M. Topham, A. Gilles, B. David, C. Folgoas, E. Moya-Leclair, et al., An engineered PET depolymerase to break down and recycle plastic bottles, Nature 580 (2020) 216–219, https://doi.org/10.1038/s41586-020-2149-4.
[13] V. Pirillo, L. Pollegioni, G. Molla, Analytical methods for the investigation of enzyme-catalyzed degradation of polyethylene terephthalate, FEBS J. 288 (2021) 4730–4745, https://doi.org/10.1111/febs.15850.
[14] Å.M. Ronkvist, W. Xie, W. Lu, R.A. Gross, Cutinase-Catalyzed hydrolysis of poly (ethylene terephthalate, Macromolecules 42 (2009) 5128–5138, https://doi.org/10.1021/ma9005318.
[15] M.R. Belisário-Ferrari, R. Wei, T. Schneider, A. Honak, W. Zimmermann, Fast Turbidimetric Assay for Analyzing the Enzymatic Hydrolysis of Polyethylene Terephthalate Model Substrates, Biotechnol. J. 14 (2019) 10–14, https://doi.org/10.1002/biot.201800272.
[16] K. Vogel, R. Wei, L. Pfaff, D. Breite, H. Al-Fathi, C. Ortmann, et al., Enzymatic degradation of polyethylene terephthalate nanoplastics analyzed in real time by isothermal titration calorimetry, Sci. Total Environ. 773 (2021), 145111, https://doi.org/10.1016/j.scitotenv.2021.145111.
[17] R. Frank, D. Krinke, C. Sonnendecker, W. Zimmermann, H.G. Jahnke, Real-Time Noninvasive Analysis of Biocatalytic PET Degradation, ACS Catal. 12 (2022) 25–35, https://doi.org/10.1021/ACSCATAL.1C03963/ASSET/IMAGES/LARGE/CS1C03963_0004.JPEG.
[18] T.B. Thomsen, C.J. Hunt, A.S. Meyer, Influence of substrate crystallinity and glass transition temperature on enzymatic degradation of polyethylene terephthalate (PET), N. Biotechnol. 69 (2022) 28–35, https://doi.org/10.1016/j.nbt.2022.02.006.
[19] J. Arnling Bååth, K. Borch, K. Jensen, J. Brask, P. Westh, Comparative Biochemistry of Four Polyester (PET) Hydrolases, ChemBioChem 22 (2021) 1627–1637, https://doi.org/10.1002/cbic.202000793.
[20] Y. Ma, M. Yao, B. Li, M. Ding, B. He, S. Chen, et al., Enhanced poly(ethylene terephthalate) hydrolase activity by protein engineering, Engineering 4 (2018) 888–893, https://doi.org/10.1016/j.eng.2018.09.007.
[21] E.Z.L. Zhong-Johnson, C.A. Voigt, A.J. Sinskey, An absorbance method for analysis of enzymatic degradation kinetics of poly(ethylene terephthalate) films, Sci. Rep. 2021 111 11 (2021) 1–9, https://doi.org/10.1038/s41598-020-79031-5.
[22] J. Arnling Bååth, K. Borch, P. Westh, A suspension-based assay and comparative detection methods for characterization of polyethylene terephthalate hydrolases, Anal. Biochem (2020) 607, https://doi.org/10.1016/j.ab.2020.113873.
[23] A.C. Chang, A. Patel, S. Perry, Y.V. Soong, C. Ayafor, H.W. Wong, et al., Understanding Consequences and Tradeoffs of Melt Processing as a Pretreatment for Enzymatic Depolymerization of Poly(ethylene terephthalate, Macromol. Rapid Commun. (2022) 2100929, https://doi.org/10.1002/marc.202100929.
[24] R.K. Brizendine, E. Erickson, S.J. Haugen, K.J. Ramirez, J. Miscall, A.R. Pickford, et al., Particle size reduction of poly(ethylene terephthalate) increases the rate of enzymatic depolymerization but does not increase the overall conversion extent, ACS Sustain Chem. Eng. 10 (2022) 9131–9149, https://doi.org/10.1021/acssuschemeng.2c01961.
[25] T.B. Thomsen, C.J. Hunt, A.S. Meyer, Standardized method for controlled modification of poly (ethylene terephthalate) (PET) crystallinity for assaying PET degrading enzymes, MethodsX 9 (2022), 101815, https://doi.org/10.1016/J.MEX.2022.101815.
[26] J. Kari, M. Andersen, K. Borch, P. Westh, An inverse michaelis-menten approach for interfacial enzyme kinetics, ACS Catal. 7 (2017) 4904–4914, https://doi.org/10.1021/acscatal.7b00838.
[27] Y. Cui, Y. Chen, X. Liu, S. Dong, Y. Tian, Y. Qiao, et al., Computational Redesign of a PETase for Plastic Biodegradation under Ambient Condition by the GRAPE Strategy, ACS Catal. 11 (2021) 1340–1350, https://doi.org/10.1021/acscatal.0c05126.
[28] J. Arnling Bååth, K. Jensen, K. Borch, P. Westh, J. Kari, Sabatier principle for rationalizing enzymatic hydrolysis of a synthetic polyester, JACS Au 2 (2022) 1223–1231, https://doi.org/10.1021/jacsau.2c00204.